Vacuum 164 (2019) 361–366

Contents lists available at ScienceDirect

Vacuum

journal homepage: www.elsevier.com/locate/vacuum

Thermal deformation behavior of the Al_2O_3-Cu/(W, Cr) electrical contacts

Xiaohui Zhang[a,b,c], Yi Zhang[a,b,c,*], Baohong Tian[a,b,c,**], Yanlin Jia[d,***], Yong Liu[a,b,c], Kexing Song[a,b,c], Alex A. Volinsky[e]

[a] School of Materials Science and Engineering, Henan University of Science and Technology, Luoyang, 471023, PR China
[b] Collaborative Innovation Center of Nonferrous Metals, Henan Province, Luoyang, 471023, PR China
[c] Henan Key Laboratory of Nonferrous Materials Science and Processing Technology, Luoyang, 471023, PR China
[d] College of Materials Science and Engineering, Beijing University of Technology, Beijing, 100124, PR China
[e] Department of Mechanical Engineering, University of South Florida, Tampa, 33620, USA

ARTICLE INFO

Keywords:
Vacuum hot-pressing sintering
Internal oxidation
Hot deformation
Dynamic recrystallization

ABSTRACT

Al_2O_3-Cu/25W5Cr and Al_2O_3-Cu/35W5Cr composites were fabricated by vacuum hot-pressing sintering and internal oxidation process. The electrical conductivity, relative density and Brinell hardness were measured. The effects of the nano-Al_2O_3 and tungsten on the Al_2O_3-Cu/(W, Cr) composites hot deformation were investigated through the isothermal compression tests using the Gleeble-1500D thermo-mechanical simulator ranging from 650 °C to 950 °C and 0.001–10 s^{-1} strain rate. The deformed microstructure was characterized and analyzed by optical and transmission electron microscopy. The interaction of work hardening, dynamic recovery and dynamic recrystallization was illustrated. It is demonstrated that Cr particles were extruded into strips; W particles underwent a slight deformation during the hot compression. Besides, the higher tungsten content composite had higher flow stress. Nano-Al_2O_3 particles pinned dislocations and inhibited the dynamic recovery and dynamic recrystallization. In addition, it is still in the stage of sub-crystals formation at 850 °C, 0.01s^{-1}. Consequently, the Al_2O_3-Cu/35W5Cr composite has typical dynamic recovery characteristic. Hence, Al_2O_3-Cu/(W, Cr) composites demonstrate outstanding high temperature performance.

1. Introduction

Electrical contacts are very common in power transmission, automatic control systems and electronic information industry. They play a significant role in making circuits, current carrying and breaking circuits in high and low voltage vacuum switches [1,2]. With upgrading the manufacturing industry and the improvement of the intelligent level, the demand for high performance electrical contacts is increasing worldwide. The physical and chemical action of high temperature, wear and arc discharge in the process of electrical contact determines that the electrical contact material must have good mechanical properties and resistance to arc erosion [3,4]. Copper matrix composites are widely used in electrical contact materials due to their good thermal conductivity and low cost. Nano-Al_2O_3 reinforced dispersion copper not only has high strength and high conductivity but also high recrystallization temperature and good thermal stability [5,6]. Lee et al. [7] used internal oxidation method to prepare dispersion copper, and a large number of alumina particles with a diameter of about 10 nm were distributed on the copper matrix. Finally, Orowan mechanism was used to explain the relationship between the microstructure and mechanical properties of dispersion copper. Besides, it has also been shown that the in situ formed nano-Al_2O_3 particles can increase the anti-stripping performance of contact materials [8]. Furthermore, the in situ formed nano-Al_2O_3 particles can effectively solves the problem of weak interfacial bonding between the ceramic reinforcing phase and the matrix. Although the dispersion copper has many advantages, the dielectric strength and breaking capacity is not satisfactory. A good way to address this problem is doping the alloy elements in the dispersion copper. Tungsten copper not only has high hardness and high voltage resistance, but also has good resistance to arc erosion, so it is widely used in high voltage circuit breaker. Studies have shown that the tungsten in the copper-tungsten contact gradually accumulates into a needle-like skeleton under the high temperature of the arc, which can restrict the flow of liquid copper with low melting point [9,10]. Cu-Cr alloy is the ideal contact material for vacuum switch, which has the characteristics of strong breaking capacity, low chopping current value and strong

* Corresponding author. School of Materials Science and Engineering, Henan University of Science and Technology, Luoyang, 471023, PR China.
** Corresponding author. Collaborative Innovation Center of Nonferrous Metals, Henan Province, Luoyang, 471023, PR China.
*** Corresponding author.
E-mail addresses: zhshgu436@163.com (Y. Zhang), bhtian007@163.com (B. Tian), jiayanlin@126.com (Y. Jia).

https://doi.org/10.1016/j.vacuum.2019.03.054
Received 14 March 2019; Received in revised form 25 March 2019; Accepted 25 March 2019
Available online 26 March 2019
0042-207X/

resistance to arc erosion, and the similar work function of Cr and Cu ensures the basic stability of the surface composition after arc erosion [11–13]. In our previous studies, tungsten particles have undergone a resintering process at high temperatures during arc erosion, gradually enriching to form needle-like structures of about 10 μm in length [14]. However, little attention has been paid to the thermal deformation behavior of the composites.

In recent years, extensive studies of electrical contact materials focuses on the arc erosion behavior, but there are few reports on the mechanical properties and thermal deformation behavior of electrical contact. Huang et al. [15] reported that the strengthening mechanism of CuW70 alloy is the work hardening caused by the slippage of copper phase. Hiraoka et al. [16] proposed that during the compression deformation of W(80)/Cu composites, the internal grains presented fibrous structure with the increase of the deformation. Due to the high temperature and energy during the arc burning, the mechanical behavior and failure mechanism of electrical contact materials are quite different from that at room temperature. In order to investigate the thermal deformation behavior and deformation microstructure evolution of the Al_2O_3-Cu/25W5Cr and Al_2O_3-Cu/35W5Cr composites, Gleeble-1500D thermal simulation testing machine was used. Finally, the deformation rules and strengthening mechanisms of nano-Al_2O_3, W and Cr particles were determined.

2. Experimental procedure

Cu-0.4 wt%Al (2–5 μm diameter, purity > 99.9%) powder, W powder (5 μm average diameter, purity > 99.9%) and Cr powder (purity > 99.9%) with an average particle diameter of 44 μm were used. Cu_2O (purity > 99.9%) powder ranging from 2 μm to 5 μm in size were served as oxygen source. Fig. 1 shows the nominal composition of the Al_2O_3-Cu/25W5Cr and Al_2O_3-Cu/35W5Cr composites. Powders were adequately mixed in a YH-10 mixer for 2 h using a ball-to-powder weight ratio of 10:1 before sintering. Copper balls were used as grinding media. Fig. 2(a) and Fig. 2(b) show the morphology of the two mixed powders characterized by the JSM-IT100 scanning electron microscope. The sintering process was conducted in a ZMY-50-15 vacuum hot-press sintering furnace. The parameters were as follows: vacuum degree was 3–4 Pa, heating rate was 10 °C/min, 15 MPa uniaxial contact pressure was applied at 650 °C and held for 1 h, continued by heating to 950 °C held for 1 h, then dropping the temperature to room temperature prior to sample removal.

After the electrical conductivity, Brinell hardness and relative density were measured, the microstructure of as-sintered samples was analyzed by the JSM-7800F field emission scanning electron microscope and the JEM-2100 transmission electron microscope. As-sintered composites were cut into size for Φ8 mm x 12 mm cylindrical specimen. Isothermal axial hot compression test was performed using the Gleeble-1500D thermal simulation testing machine. The deformation temperature was set at 650 °C, 750 °C, 850 °C and 950 °C, the strain rate was 0.001s^{-1}, 0.01 s^{-1}, 0.1 s^{-1},1 s^{-1} and 10 s^{-1}, heating rate was 10 °C/s. In order to make the sample temperature uniform, the sample was kept warm for 3–5 min in advance, and then isothermal axial compression was started. After the deformation, the samples were quickly taken out and cooled by water quenching to retain the high-temperature structure. All the experiment process was shown in Fig. 2(c).

3. Result

3.1. The comprehensive properties of the Al_2O_3-Cu/(W, Cr) composites

Fig. 3 shows the comprehensive properties of the two contact materials. The relative density of the two composites was above 97%. As more content of tungsten was added into the composite, the Brinell hardness increased from 102.3 HBW to 126.8 HBW. On the contrary, the electrical conductivity decreased from 67.28 %IACS to 62.20 % IACS. A large number of high hardness W particles were distributed on the matrix, and strengthening took place due to the “carrying more applied load” effect by the stiffness W particles [17]. Furthermore, hindering the dislocations movement can also increase the hardness of the composites. This strengthening mechanism can be illustrated in Fig. 7.

3.2. Microstructure

Figure 4 shows the optical microscope images of the two composites before and after the hot compression. It can be seen from Fig. 4(a and b) that the as-sintered samples have a compact structure without obvious holes and other defects. Cr (large particles) and W (small particles) were evenly distributed on the dispersion copper matrix, and no obvious agglomeration occurred. Fig. 4(c and d) and Fig. 4(e and f) are the microstructures of the two samples, which were deformed at 850 °C, 0.01 s^{-1} and 1 s^{-1}, respectively. As can be seen from Fig. 4, with the increase of the strain rate, the grains gradually become slender and narrow, and Cr particles were extruded into strips, which were elongated perpendicular to the compressed direction. Due to its high hardness, the deformation of W particles was not obvious under the two conditions. In order to clarify the deformation of W particles in the Al_2O_3-Cu/35W5Cr composite, the transmission electron microscopy was used. The result was shown in Fig. 7.

3.3. True stress-true strain curves

Figure 5 shows the true stress-true strain curves of the two composites under different conditions. Based on the different trends of the curves, it indicates the plastic deformation mechanism. When the deformation temperature is constant, the flow stress increases with the strain rate. In general, in the initial stage of thermal deformation, with the generate of the glide dislocations, the surface of the samples, the grain boundary, and other stress concentrations are acting prior to causing dislocations propagation. After the rapid rise of dislocations density, dislocations tangle will increase the resistance of dislocations and produce work hardening. When the second stage of work hardening motivate, a substantial amount of dislocation jog are produced resulting

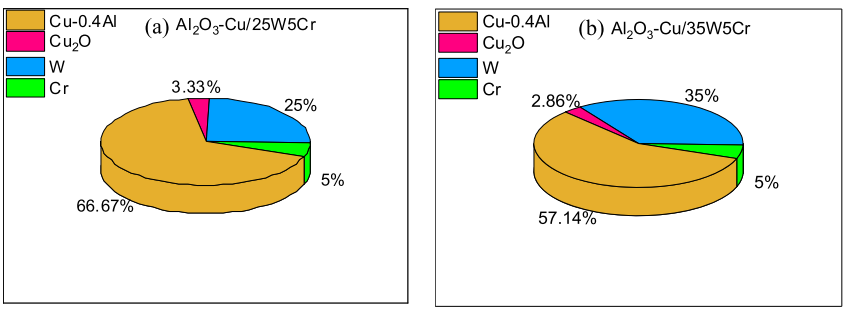

Fig. 1. The composition of: (a) Al_2O_3-Cu/25W5Cr and (b) Al_2O_3-Cu/35W5Cr composites.

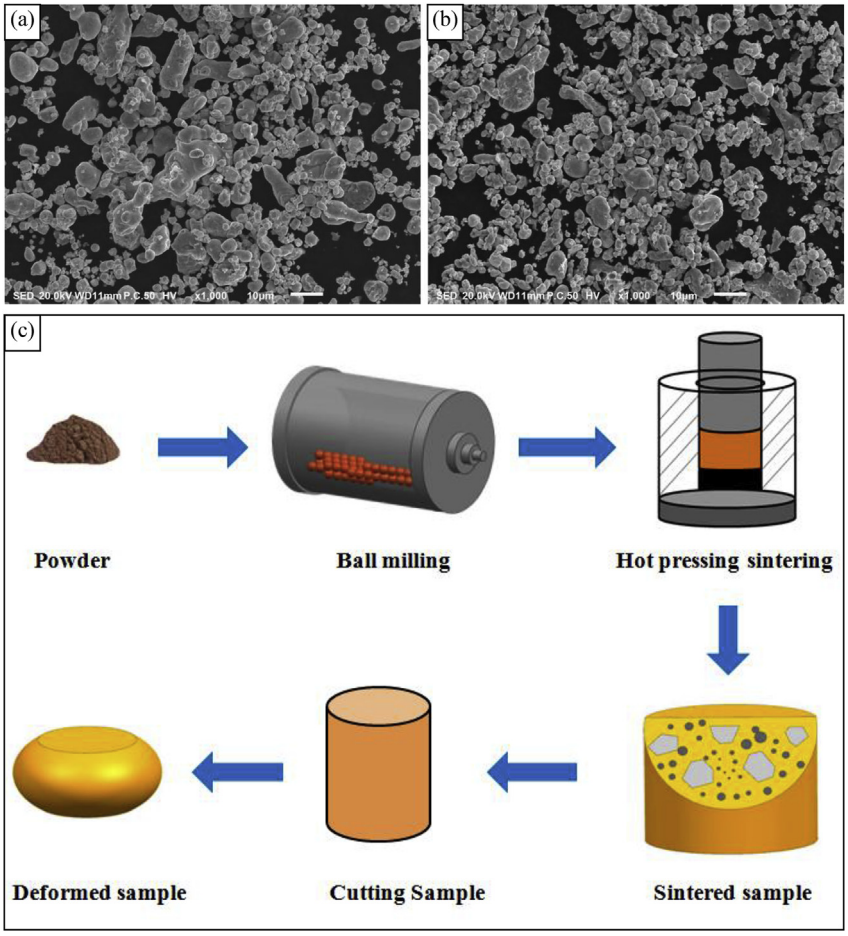

Fig. 2. SEM images of mixed powder and schematics of the experimental procedure. (a) Morphology of the Al_2O_3-Cu/25W5Cr mixed powder; (b) Morphology of the Al_2O_3-Cu/35W5Cr mixed powder; (c) Schematics of the experimental procedure.

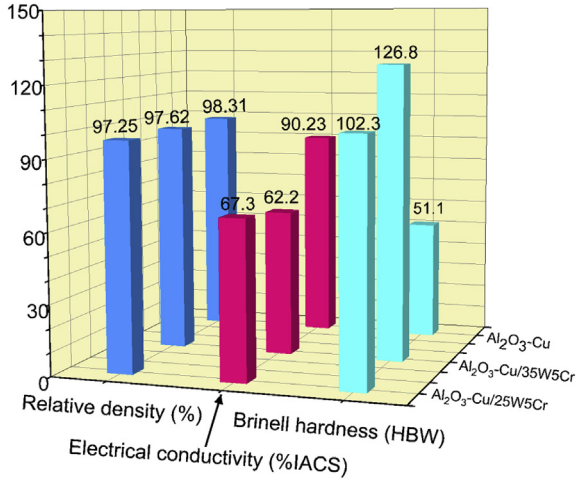

Fig. 3. Comprehensive properties of the Al_2O_3-Cu/(W, Cr) composites.

in the increasing of the flow stress until a peak occurs. However, the resistance caused by the formation of dislocation jog is sensitive to the temperature. This means that the intensification of atomic thermal motion will reduce the resistance of the movement of jog. Hence, the flow stress gradually decreases and tends to be stable. In general, the main mechanism of this process are dynamic recovery and dynamic recrystallization. In the process of dynamic recovery, the cross slip and climb of dislocations play a significant role, which include the defect density decreasing, the inverse dislocations neutralizing, and the dislocations rearranging, which was defined as polygonization [18–20]. Besides, dynamic recrystallization can be achieved by nucleation and growth of grains to eliminate dislocations and subgrain boundaries in deformed matrix. Increasing the temperature or decreasing the strain rate are conducive to the occurrence of the dynamic recrystallization. During high temperature deformation, the stress-strain behavior of the material depends on the balance among the work hardening, dynamic recovery and dynamic recrystallization [21].

The strain rate corresponding to Fig. 5(a) and Fig. 5(c) is $0.01s^{-1}$. Both curves have typical dynamic recrystallization characteristics. At the initial stage of deformation, the stress rises sharply. A peak value emerges in a very short time. Afterwards, the flow stress decreases slightly until a steady value is reached. Consequently, dynamic recrystallization dominates the dynamic softening. The boundary of recrystallized grains migrates rapidly, and the dislocation density within grains decreases. Consequently, the effect of work hardening reduces [22–24]. Therefore, the stress-strain curves possess obvious peak stress. For comparison, the strain rate of Fig. 5(b) and (d) are $1\ s^{-1}$. Compared with the low strain rate curves in Fig. 5(a) and (c), all curves exhibit similar trends, which are related to deformation temperature and strain rate. The flow stress increases with lower temperature or higher strain rate. At the initial stage of deformation, the stress also rises sharply. Then it presents the similar trends with the Fig. 5(a) and (c). The dynamic recrystallization characteristics were presented in Fig. 5(b) and (d). It is attributed to the low stacking fault energy of copper in the Al_2O_3-Cu/(W, Cr) composites. The cross-slip ability of dislocations is poor. Consequently, the dynamic recovery was inhibited. The high angle grain boundary was easy to generate. Thus, the dynamic

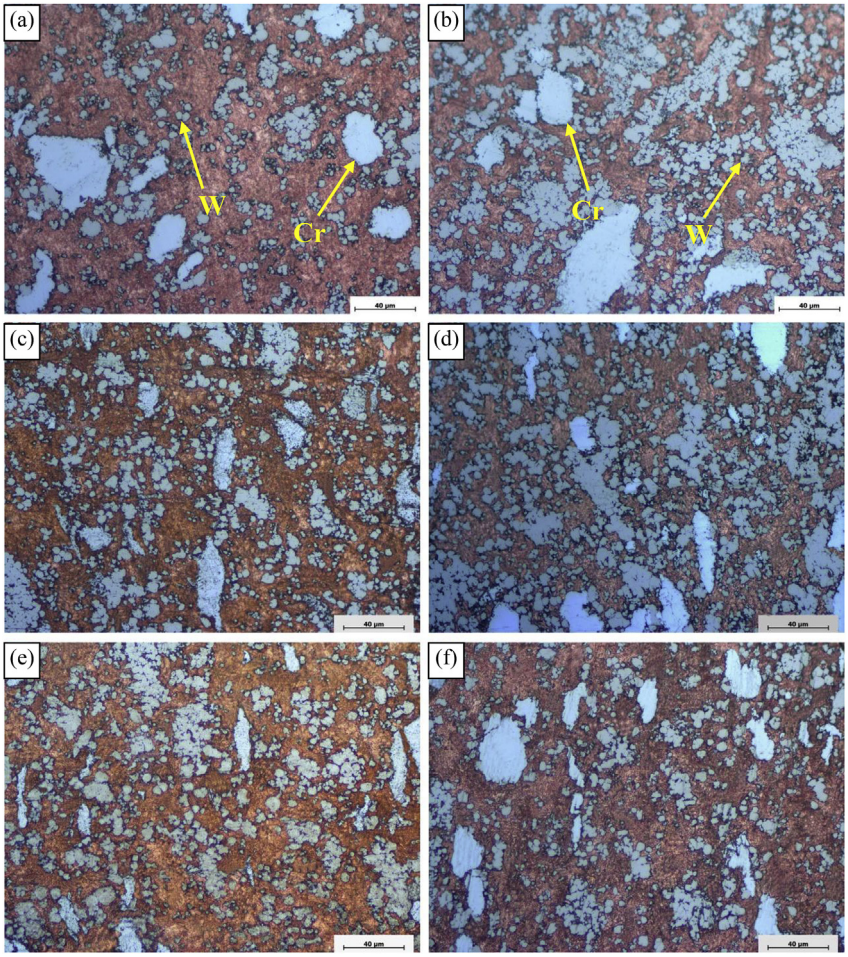

Fig. 4. The optical microscope images of the two composites at different conditions: (a) As-sintered Al_2O_3-Cu/25W5Cr; (b) As-sintered Al_2O_3-Cu/35W5Cr; (c) Al_2O_3-Cu/25W5Cr deformed at 850 °C, 0.01 s^{-1}; (d) Al_2O_3-Cu/35W5Cr deformed at 850 °C, 0.01 s^{-1}; (e) Al_2O_3-Cu/25W5Cr deformed at 850 °C, 1 s^{-1}; (f) Al_2O_3-Cu/35W5Cr deformed at 850 °C, 1 s^{-1}.

recrystallization took place. In addition, compared with the Al_2O_3-Cu/25W5Cr and Al_2O_3-Cu/35W5Cr composites, at the same deformation condition, higher tungsten content composite possess the higher flow stress, which suggest that the W particles have certain hindering effect on the movement of dislocation. These results agree with the analysis results of TEM characterization in Fig. 7.

3.4. Evolution of deformation structure

To further demonstrate the deformation microstructure evolution, TEM characterization was performed. In the process of thermal deformation, due to the effect of work hardening, the gliding dislocations were generated at the stress concentration such as grain boundary. As shown in Fig. 6(a), The sample possessed obvious dynamic recovery characteristics after thermal compression at 850 °C, 0.01s^{-1}. By analyzing the diffraction spots of the subgrains on both sides of the sub-boundary in Fig. 6(a), it illustrated that misorientation of subgrains was about 0.7°. In addition, the sample was in the stage of dynamic recovery as shown in Fig. 6(b). Furthermore, the sub-boundary was consist of dislocation walls, and the dislocation walls had a discrepant width. For example, the dislocation wall in e1 zone was wider, and network structure attribute to dislocation tangle was observed. However, the dislocation wall in e2 zone became narrowed, and the dislocation configuration was difficult to distinguish. Besides, the matrix in both sides of the sub-boundary had a mass of dislocation tangle and dislocation cell. For instance, a large number of dislocations were pinned by the nanoparticles resulting in dislocation tangle in e3 zone. According to the selected area electron diffraction pattern, the particles were nano-Al_2O_3.

3.5. The deformation of tungsten

A series of analysis was performed on the deformation of W particles and the surrounding matrix during the thermal deformation process. As shown in Fig. 7(a), a large number of dislocations were gathered around W particle and dislocation tangle was formed. In addition, although tungsten has high hardness, some researches have indicated the deformation behavior of tungsten alloys. Woodward et al. investigated the true strain rate effects on the flow stress of the heave tungsten alloys, and it indicated that softening could take place at high strain rate [25]. Lee et al. [26] reported that a decrease in the strain rate sensitivity was observed when the temperature was above 700 °C. Karl proposed that the tungsten-copper alloy undergone ductile-brittle transition at 400 °C [27]. It can be seen from Fig. 7(b) that there is a slight deformation at the edge of W particle. This phenomenon can be illustrated that the movement of plenty of dislocations at the interface is impeded by W particle, and the stress is generated by the dislocation pile-up. Further analysis demonstrated that a large amount of dislocations were stimulated in the W particle, as shown in Fig. 7(c and d).

4. Conclusion

The Al_2O_3-Cu/(W, Cr) composites were fabricated by vacuum hot-pressing sintering process. Hot deformation tests were employed at

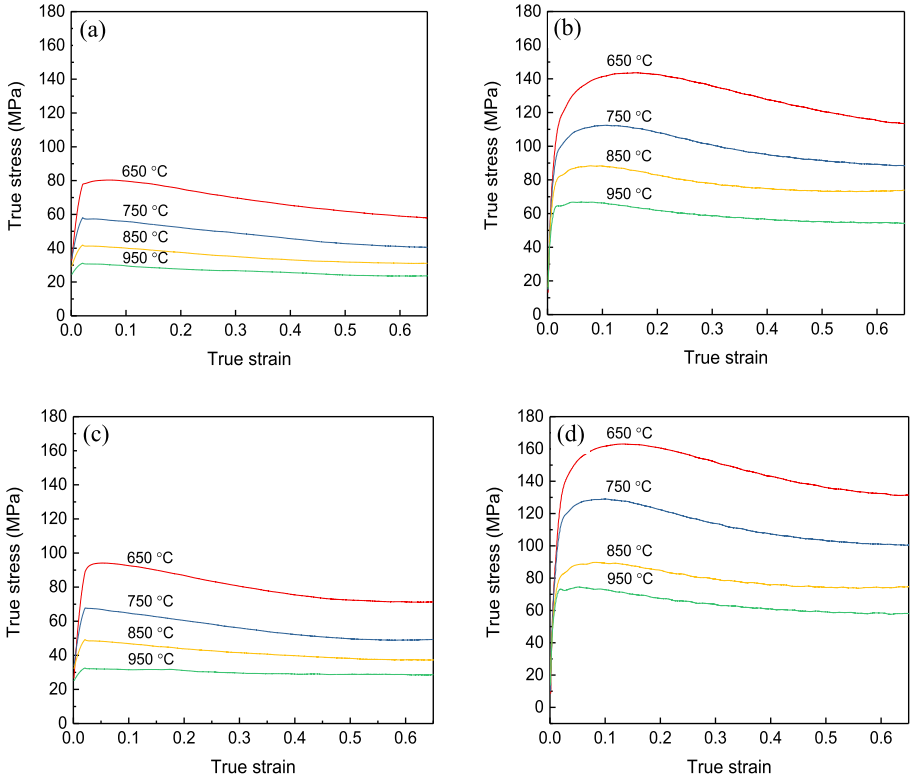

Fig. 5. True stress-true strain curves of Al_2O_3-Cu/(W, Cr) electrical contacts deformed at 850 °C and different strain rates: (a) Al_2O_3-Cu/25W5Cr deformed at 0.01 s^{-1}; (b) Al_2O_3-Cu/25W5Cr deformed at 1 s^{-1}; (c) Al_2O_3-Cu/35W5Cr deformed at 0.01 s^{-1}; (d) Al_2O_3-Cu/35W5Cr deformed at 1 s^{-1}.

temperature ranging from 650 °C to 950 °C and the strain rate 0.001–10 s^{-1}. The conclusions are as follows:

Cr particles were extruded into strips, which were elongated perpendicular to the compressed direction during the hot compression. The flow stress increased with the increase of strain rate, and decreased with the increase of deformation temperature. Besides, the Al_2O_3-Cu/35W5Cr composite possessed a higher flow stress at the same deformation conditions. Nano-Al_2O_3 particles pinned dislocations and inhibited the dynamic recovery and dynamic recrystallization. Consequently, it was still in the stage of sub-crystals formation at 850 °C, 0.01s^{-1}. W particles underwent a slight deformation during the hot compression.

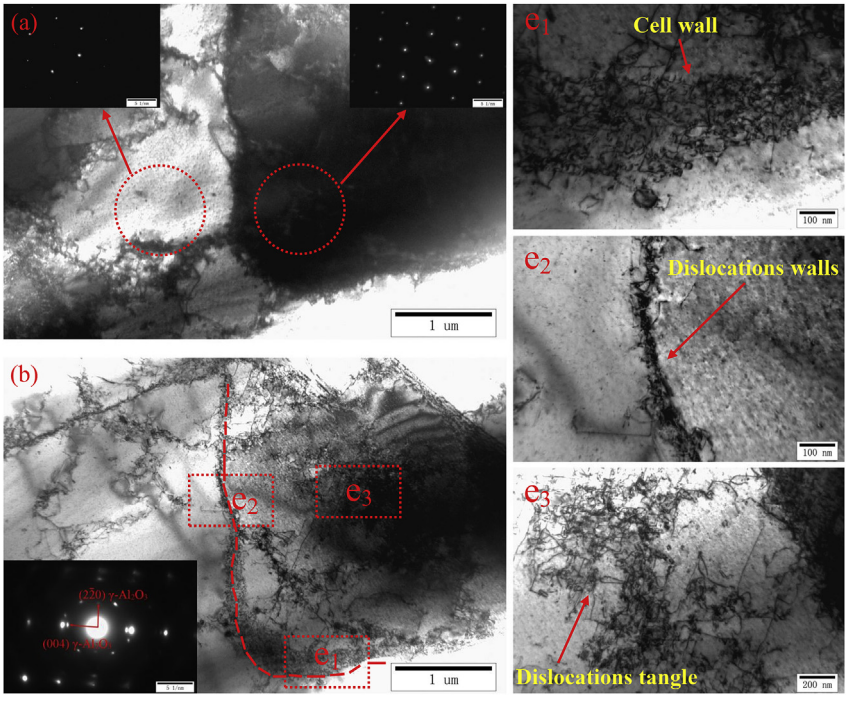

Fig. 6. TEM images of the deformed Al_2O_3-Cu/35W5Cr sample: (a) Sub-grains; (b) Dislocation walls.

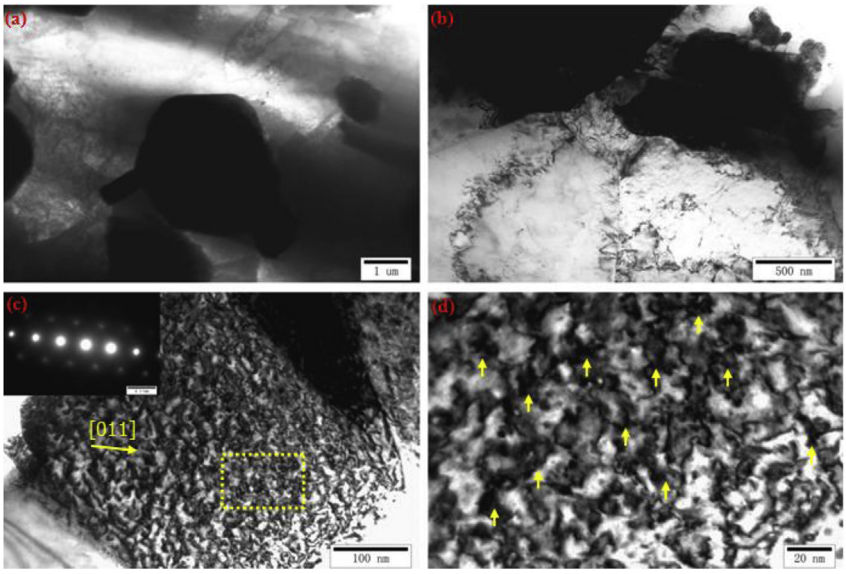

Fig. 7. TEM images of the deformed tungsten particles: (a) Dislocation tangle near tungsten particle; (b) A slight deformation at the edge of tungsten particle; (c) Dislocations in tungsten; (d) Magnified region of (c).

Acknowledgments

This work was supported by the Open Cooperation Project of Science and Technology of the Henan Province (182106000018), the Henan University Scientific and Technological Innovation Talent Support Program (18HASTIT024) and the National Natural Science Foundation of China (U1704143).

References

[1] I.H. Sung, J.W. Kim, H.J. Noh, H. Jang, Effect of displacement and humidity on contact resistance of copper electrical contacts, Tribol. Int. 95 (2016) 256–261.
[2] N. Ray, B. Kempt, T. Mutzel, L. Froyen, K. Vanmeensel, J. Vleugels, Effect of WC particle size and Ag volume fraction on electrical contact resistance and thermal conductivity of Ag-WC contact materials, Mater. Des. 85 (2015) 412–422.
[3] X.C. Huang, Y. Feng, G. Qian, K. Liu, Erosion behavior of Ti3AlC2 cathode under atmosphere air arc, J. Alloy. Comp. 727 (2017) 419–427.
[4] M. Zhen, H.R. Geng, M.M. Li, G.L. Nie, J.F. Leng, Effects of Y2O3 on the property of copper based contact materials, Composites Part B 52 (2013) 51–55.
[5] W.J. Li, W.Z. Shao, N. Xie, Z. Lu, Y.R. Li, M.S. Yang, B.A. Chen, Q. Zhang, Q. Wang, L. Zhen, Air arc erosion behavior of CuZr/Zn2SnO4 electrical contact materials, J. Alloy. Comp. 743 (2018) 697–706.
[6] S. Bera, W.M. Lojkowsky, Development of wear-resistant Cu-10Cr-3Ag electrical contacts with alloying and high pressure sintering, Metal Mat. Trans. A Phys. Metall. Mat. Sci. 40 (2009) 3276–3283.
[7] J.S. Lee, Y.C. Kim, S. Lee, N.J. Kim, Correlation of the microstructure and mechanical properties of oxide-dispersion-strengthened coppers fabricated by internal oxidation, Metall. Mater. Trans. 35 (2004) 493–502.
[8] D.P. Lu, J. Jiang, L. Lu, X.J. Liao, K.M. Nesterov, R.K. Islamgaliev, R.Z. Valiev, K.M. Liu, Hardness, electrical conductivity and thermal stability of externally oxidized Cu-Al_2O_3 composite processed by SPD, J. Mater. Eng. Perform. 26 (2017) 2110–2117.
[9] E.D. Taylor, Cathode spot behavior on Tungsten –copper contact in vacuum and the effect on erosion, Electr. Contacts Proc. Annu. Holm. Conf. Electr. Contacts (2005) 135–138.
[10] Q.Y. Chen, S.H. Liang S, F. Wang, L.C. Zhuo, Microstructural investigation after vacuum electrical breakdown of the W-30wt.%Cu contact material, Vacuum 149 (2018) 256–261.
[11] Y.L. Chang, W. Zheng, Z.M. Zhou, Y.X. Zhai, Y.P. Wang, Preparation and performance of Cu-Cr contact materials for vacuum switches with low contact pressure, J. Electron. Mater. 45 (2016) 5647–5654.
[12] C. Nicolle, D. Mazzucchi, J.P. Gauthier, F. Gentils, Behavior of CuCr and WCu contacts during making tests at high voltage and high currents, Proc. Int. Symp. Discharge. Electr. Insul. Vac.IEEE (2010) 261–264.
[13] S.X. Zhu, Y. Liu, B.H. Tian, Y. Zhang, K.X. Song, Arc erosion behavior and mechanism of Cu/Cr20 electrical contact material, Vacuum 143 (2017) 129–137.
[14] X.H. Zhang, Y. Zhang, B.H. Tian, J.C. An, Z. Zhao, A.A. Volinsky, Y. Liu, K.X. Song, Arc erosion behavior of the Al_2O_3-Cu/(W, Cr) electrical contacts, Composites Part B 160 (2019) 115–122.
[15] Y.T. Huang, W.Z. Chen, D.P. Tang, Study on microstructure and properties of CuW70 alloy under dynamic and static deformation, Heat Treat. Met. 32 (2007) 258–262.
[16] Y. Hiraoka, H. Hanado, T. Inoue, Deformation behavior at room temperature of W–80 vol% Cu composite, Int. J. Refract. Metals Hard Mater. 22 (2004) 87–93.
[17] N. Chawla, Y.L. Shen, Mechanical behavior of particle reinforced metal matrix composites, Adv. Eng. Mater. 3 (2001) 357–370.
[18] E.O. Hall, The deformation and ageing of mild steel: III discussion of results, Proc. Phys. Soc. B 64 (1951) 747–753 (1951).
[19] A. Misra, J.P. Hirth, H. Kung, Single-dislocation-based strengthening mechanisms in nanoscale metallic multilayers, Philos. Mag. A 82 (2002) 2935–2951 (2002).
[20] J.J. Gilman, Structure and polygonization of bent zinc monocrystals, Acta Metall. 3 (1955) 277–288.
[21] B.J. Wang, Y. Zhang, B.H. Tian, J.C. An, A.A. Volinsky, H.L. Sun, K.X. Song, Effects of Ce addition on the Cu-Mg-Fe alloy hot deformation behavior, Vacuum 155 (2018) 594–603.
[22] J.J. Jonas, C.M. Sellars, W.J. McG. Tegart, Strength and Structure under Hot-Working Conditions vol. 14, (1969), pp. 1–24.
[23] K.C. Le, Q.S. Nguyen, Polygonization as low energy dislocation structure, Continuum Mech. Therm. 22 (2010) 291–298.
[24] T. Sakai, J.J. Jonas, Dynamic recrystallization: mechanical and microstructure considerations, Acta Metall. 32 (1984) 189–209.
[25] R.L. Woodward, N.J. Baldwin, B.J. Baxter, Effect of strain rate on the flow stress of three liquid phase sintered tungsten alloys, Metall. Trans. A 16 (1985) 2031–2037.
[26] W.S. Lee, G.L. Xiea, C.F. Lin, The strain rate and temperature dependence of the dynamic impact response of tungsten composite, Mater. Sci. Eng. 257 (1998) 256–267.
[27] M.H. Karl, Material Science and Technology vol. 8, Science Press, Beijing, 1999, pp. 525–530.